AIP | Journal of Applied Physics

Development of a cost effective surface-patterned transparent conductive coating as top-contact of light emitting diodes

Arpita Haldar, Susanta Bera, Sunirmal Jana, Kallol Bhattacharya, and Rajib Chakraborty

Citation: Journal of Applied Physics **115**, 193108 (2014); doi: 10.1063/1.4876737
View online: http://dx.doi.org/10.1063/1.4876737
View Table of Contents: http://scitation.aip.org/content/aip/journal/jap/115/19?ver=pdfcov
Published by the AIP Publishing

Development of a cost effective surface-patterned transparent conductive coating as top-contact of light emitting diodes

Arpita Haldar,[1,2] Susanta Bera,[2] Sunirmal Jana,[2,a)] Kallol Bhattacharya,[1] and Rajib Chakraborty[1,a)]
[1]*Department of Applied Optics & Photonics, University of Calcutta, Kolkata-700009, India*
[2]*Sol-Gel Division, CSIR-Central Glass and Ceramic Research Institute, Kolkata 700032, India*

(Received 22 November 2013; accepted 4 May 2014; published online 20 May 2014)

Sol-gel process has been used to form indium zinc oxide films using an optimized combination of zinc to indium concentration in the precursor solutions. Different structures, like one (1D) and two-dimensional (2D) gratings and diffractive optical elements (DOEs) in the form of Fresnel lens are fabricated on the film surface of proposed top metal contact of LED by imprint soft lithography technique. These structures can enhance the LED's light extraction efficiency (LEE) or can shape the output beam pattern, respectively. Several characterizations are done to analyze the material and structural properties of the films. The presence of 1D and 2D gratings as well as DOEs is confirmed from field emission scanning electron and atomic force microscopes analyses. Although, X-ray diffraction shows amorphous nature of the film, but transmission electron microscopy study shows that it is nano crystalline in nature having fine particles (~8 nm) of hexagonal ZnO. Shrinkage behaviour of gratings as a function of curing temperature is explained by Fourier transform infra-red spectra and thermo gravimetric-differential thermal analysis. The visible transmission and sheet resistance of the sample are found comparable to tin doped indium oxide (ITO). Therefore, the film can compete as low cost substitute of ITO as top metal contact of LEDs.
 [http://dx.doi.org/10.1063/1.4876737]

I. INTRODUCTION

Light Emitting Diodes (LEDs) are being widely used in modern days because of its energy saving and environment friendly nature. They are used in solid state lighting, back-light units of liquid crystal displays, different colored illumination panels, traffic signals, etc. Future demands of these and advanced applications require improvement of luminous efficiency, optimal conversion of LED output into required light distribution and reduction in size and cost.[1–4] But conventional LEDs have very poor light output efficiency because of two reasons, viz., total internal reflection at the interface of active layer with surroundings and progressive absorption of the propagating light originated in the active layer.[3–7] They also use conventional optics for beam shaping. Although the internal quantum efficiency of the LEDs have improved these days, but Light Extraction Efficiency (LEE) of conventional LEDs is still very poor. A number of solutions have been proposed to solve this problem. A transparent polymer can be affixed over the device to create a larger escape angle to air.[8] Another way to improve light output is to roughen or to pattern transmission grating[5,9–13] on the emission surface that offers the trapped light more angles of escape. Grating structures of various shapes like pyramidal, spherical, conical, sinusoidal, cylindrical, and so on can be studied, but only a few can be fabricated with great success.[14–17] To obtain required light distribution, beam shaping is now done by monolithic integration of surface microstructures in the form of Diffractive Optical Elements (DOEs) which are cost-effective and results in shrinkage of overall package size and assembly costs. DOEs are usually planar and are fabricated directly on LED at wafer level with lithographic and micromechanical methods.

However, the fabrication of these structures with a different material over the top contact metal layer leads to an increased resistance[18,19] and this problem can be solved if the top contact layer is itself patterned to form the required structure. As top metal contact of LED, Transparent Conducting Oxides (TCOs), which are degenerately doped semiconductor oxides transparent to visible light, are used.[20] As TCOs, In_2O_3:Sn (ITO) dominates the market with conductivity of 1000–5000 S/cm and an optical transparency of 85–90%.[20,21] However, the limited availability of indium sources and general lack of infrastructure to recycle significant quantities of the metal result in ever-increasing price of indium which urged researchers to search for indium-free/reduced TCOs.[22–24] The co-substitution chemistry of ZnO and SnO_2 (two relatively inexpensive materials) in In_2O_3 has been explored.[25] The indium-oxide-doped ZnO (IZO) is another transparent conducting oxide which has high transparency and good electrical conductivity. The IZO films have been deposited using variety of techniques such as sputtering, pulsed laser deposition (PLD), metal organic chemical vapor deposition (MOCVD), and spray pyrolysis.[26–29]

In this work, sol-gel process has been used to form IZO film using an optimized combination of ZnO and In_2O_3 that can act as top metal contact of LED. The sol-gel technique offers the possibility of preparing a small as well as large-area coating of thin films at low cost. There is no need of sophisticated and costly equipment for fabricating IZO like that required in Refs. 26–28. It is seen that the film has

[a)]Authors to whom correspondence should be addressed. Electronic addresses: sjana@cgcri.res.in and srirajib@yahoo.com.

conductivity and optical transparency comparable to ITO, but as the percentage of indium is less in this case than ITO, material cost is comparatively less. Thereafter, grating structures of different shapes and DOEs have been fabricated by patterning the proposed top contact layer of the LED by combining imprint technique with replicated polydimethylsiloxane (PDMS) soft mold stamp. Although specific structures dedicated to this application are yet to be implemented and tested for light extraction efficiency and improvement of optical output distribution, some sample structures have been implemented and characterized. The patterning process has the advantages of high-throughput, low cost and simplicity with potential applications in electronics and photonics industries. The combination of low cost and large area process with the indium-zinc oxide material will give a new way for the large-scale fabrication of patterned TCOs for increasing light extraction efficiency and beam shaping in LED.

II. FABRICATION OF SURFACE PATTERNS

Different structures, which include 1D and 2D grating structures and Fresnel lens structure, are produced on thin film of the proposed top-contact material of LED, which is basically IZO, using sol-gel technique followed by imprint patterning. It is a four step process consisting of preparation of precursor solution, deposition of its thin film onto the soda lime silica glass substrate, fabrication of pattern onto the thin film and finally thermal annealing of the patterned film. The precursor solution has been prepared from zinc acetate dihydrate (ZA) and hydrated indium nitrate in water as solvent and acetyl acetone as solution stabilizing agent. The whole process is discussed in details by the authors in a separate report.[30] In the present work, the percentage of indium content is 60 at. % with respect to Zn in the precursor solution. 1D grating structures are prepared using PDMS stamp containing negative replica of a grating like structure available in commercial compact disc (CD) as master similar to that reported in Ref. 31. The step-by-step representation of the patterning process along with pictures of the patterns formed on glass substrate is shown in Fig. 1. The fabrication of two-dimensional grating is a two-step process. To carry out the second-step, a different PDMS stamp is superimposed in the similar manner as that of the first step. After a few minutes of the first step of grating fabrication, the next stamp is pressed perpendicularly in conformal contact between the first-step grating film and stamp. Utmost care is taken so that in the second-step, the intersection angles between the two-sets of gratings can be controlled to obtain the desired shape. After keeping the pressure for a few seconds, the stamps are carefully peeled off. The substrates with the printed 2D surface patterns are dried initially at 100 °C for 1 h and then finally cured at 450 °C. The Fresnel lens structure is also prepared on the same material coated substrate using the same procedure. Only the diffractive optical element (DOE) containing 16 such lenses are taken as the master for soft imprint patterning. Recently, microlens array have been prepared using similar technique[32] but to the best of author's knowledge, fabrication of Fresnel lens on TCO is not reported earlier.

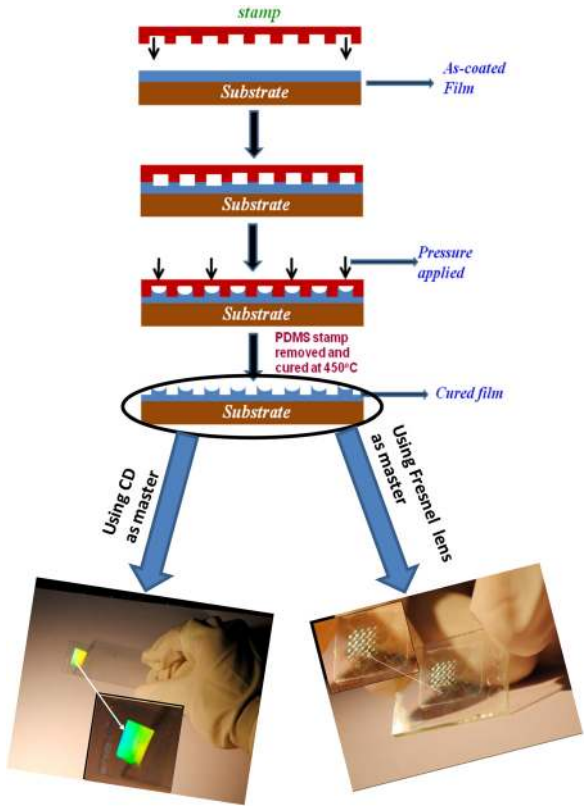

FIG. 1. Schematic of step-by-step representation of surface patterning along with pictures of formed grating patterns and Fresnel lens array.

III. CHARACTERIZATION

The sol-gel produced material is characterized to study its formation process and to evaluate its capability as a cost effective replacement of ITO as top metal contact of LED. The nature of the fabricated patterns which can enhance the LEE and assist in beam shaping is studied using different characterization techniques. Physical thickness and refractive index (at 632.8 nm wavelength) of the coatings are measured using a auto gain Ellipsometer (Gaertner make, model L116B, USA) at 70° angle of incidence having He–Ne laser as its source. The measured film thickness and refractive index are found to be 100 nm and 1.777, respectively. Thermal characteristics [Thermo Gravimetric Analysis (TGA) and Differential Thermal Analysis (DTA)] of the gel to oxide transformation in the gel film is carried out by using a Netzsch STA 409 C/CD Thermoanalyzer with Al_2O_3 as a reference material maintaining heating rate of 10 K/min in air. The chosen maximum temperature is 1000 °C. Practically, the gel film (obtained after drying at ~100 °C) material (~11 mg obtained from a series of coated samples) is taken out from the surface of the substrate by scrubbing which is used as the material for TGA-DTA experiment. Crystalline phase of the film is identified by X-ray Diffraction (XRD) study and is done by Rigaku Smartlab using CuK_α radiation (at 1.5406 Å) operating at 9 kW in the diffraction angle (2θ) from 25° to 70°. Surface morphology and the cluster size distribution of the patterned and unpatterned nanostructure films are studied by Field Emission Scanning Electron Microscopy (FESEM) (ZEISS, SUPRA^{TM}35VP) and Transmission Electron Microscopy (TEM) (TecnaiG^2 30.S-Twin, FEI Company,

Netherlands), respectively. Carbon coated 300 mesh Cu grid is used for TEM analysis. The vacuum level for this experiment is around 10^{-9} Torr. For sample preparation, the film is scratched off which is then dispersed in cyclohexane followed by ultrasonication for about 2 h. Finally, it is carefully placed on the Cu-grid. The excess liquid is allowed to evaporate in air. The grids with the sample are examined with ultra-high resolution (UHR) pole-piece using a LaB6 filament. The operated accelerating voltage and the camera length are 300 kV and 55 cm, respectively. All the patterned films are characterized by Atomic Force Microscope (AFM) using a (Nanonics, Israel make) NSOM AFM machine. The line scan images and their respective profiles are recorded. FTIR spectra of the films are measured by Thermo Electron Corporation make Nicolet 5700 FTIR spectrometer. Number of scans for each experiment was 100 while the wavenumber resolution is 4 cm^{-1}. The transmission spectra of the unpatterned and patterned films are measured by UV-VIS-NIR Spectrophotometer (Shimadzu make UV-3101-PC, Japan). The double beam scanning is used for the measurement in the wavelength range from 200 to 800 nm (photometric accuracy; ±0.3%, resolution, 0.10 nm). The nature of the grating profile is also verified from its diffraction pattern. The sheet resistances of the films are measured by two probe method using a Philips (PM 2525) make Multimeter. The resistivity and conductivity can be measured from the corresponding sheet resistance and physical thickness values.

IV. RESULTS AND DISCUSSION

A. Morphology of the patterns and microstructural properties of film

Figure 2 shows the FESEM image of the patterned indium zinc oxide thin film. It is to be noted that the indium concentration of 30, 40, 50, 55, and 60 at. % with respect to Zn in the precursor solutions have been used for indium zinc oxide film formation. Accordingly, the deposited thermally cured (450 °C) films are designated as ZI30, ZI40, ZI50, ZI55, and ZI60, respectively. Clusters of white oxide, however, appear and their nature varies with the change in percentage of indium and has been studied in details and reported in Ref. 30. These clusters are not present on the thin film (film size: length, 25 mm and width, 20 mm) derived from the precursor solutions containing 60 at% indium. As top transparent contact, smooth surface is preferred and so in this work, only this composition has been used. Fig. 2(a) shows the film having both patterned and non-patterned portion, while Figs. 2(b) and 2(c) show the 1D and 2D grating structures, respectively, and Fig. 2(d) shows the image of DOE in the form of a Fresnel lens. For 2D grating, uniform two-dimensional patterns can be seen whose pitch in the two directions depends on the placement of the mask during processing. The AFM pictures along with their line scan plot shown in Figs. 3 and 4 give a better idea about the nature of the structure and their surface quality. In Figs. 3(a)–3(c), AFM images on 1D gratings formed at different annealing temperatures are shown. In this work, gratings formed after annealing at 450 °C is considered and is shown in Fig. 3(c). Its line scan images show that the profile is sinusoidal in nature. Getting a sinusoidal grating profile by any fabrication process is not very easy. Here, the sinusoidal grating is obtained by suitably modifying the curing temperature during thermal annealing of the pattern. It is also seen that the grating height decreases with the increase of curing temperature. The peak height shrinkage might be due to removal of organics and collapsing of pores in the sol-gel thin film as can be explained from the different analysis given below. The line scan also shows a periodic 1–D strip with periodicity ~1.5 μm, similar to the master CD used for embossing.

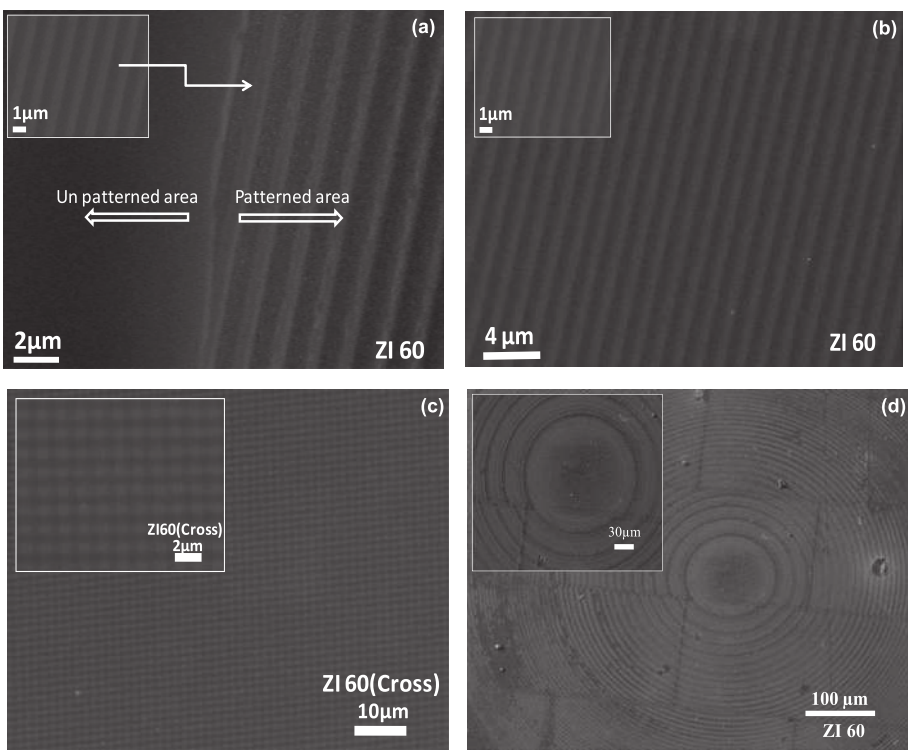

FIG. 2. FESEM images of (a) film containing patterned and non-patterned portion, (b) 1D grating pattern, (c) 2D grating pattern, (d) portion of Fresnel lens pattern. Insets show the images at higher magnification.

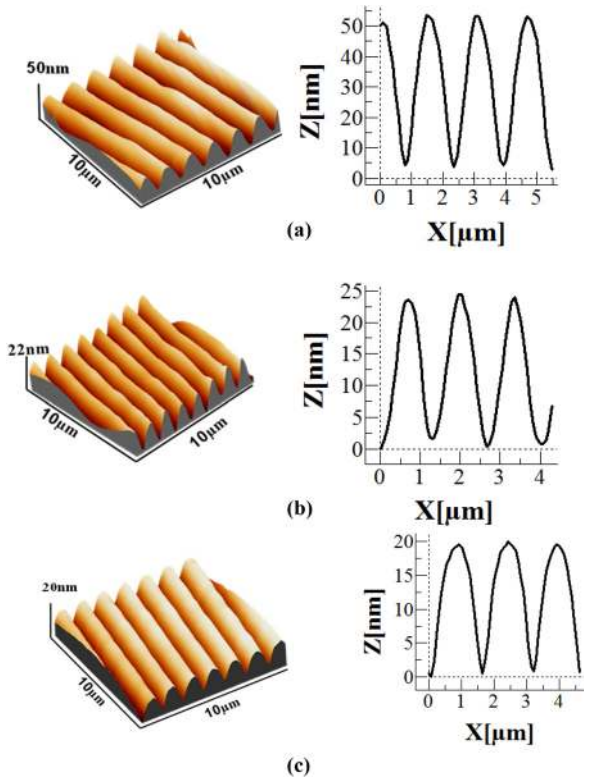

FIG. 3. AFM images along with their line scan plot of 1D grating formed with 60% Indium concentration at curing temperature of (a) 150 °C, (b) 300 °C, (c) 450 °C.

The AFM image of 2D grating formed after curing at 450 °C is shown in Fig. 4(a) along with its line scan plot. The line scan plots in the two directions are similar and so only the plot in one direction is shown here. It is seen that the height of the fabricated grating are suitable for OLED use. The AFM image of a portion of the fabricated Fresnel lens is shown in Fig. 4(b). The line scan clearly gives the idea of the profile of the lens.

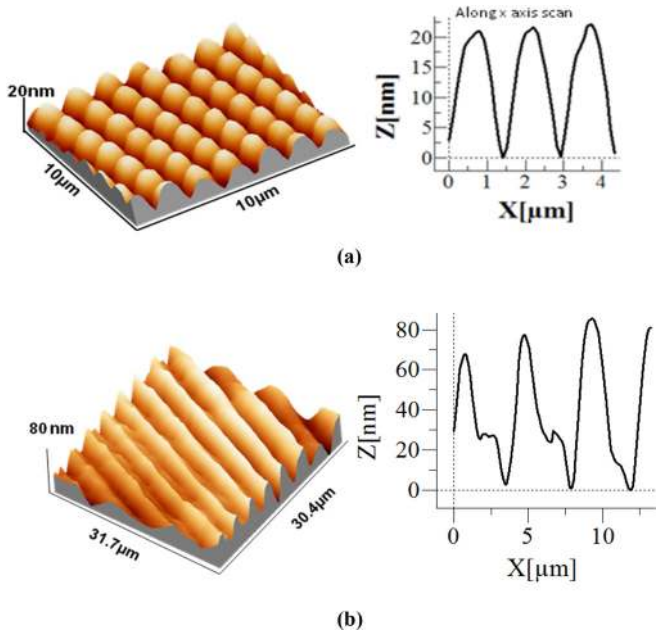

FIG. 4. AFM image along with their line scan plot of (a) 2D grating (b) portion of Fresnel lens formed with 60% indium concentration and curing temperature of 450 °C.

TEM image of the film cured at 450 °C shows agglomerated particles (average size, 7.9 nm as obtained from the histogram for the particle size distribution). The particles are seemed to be spread on the bed of amorphous materials. Although, XRD shows the film is amorphous character but the presence of distinct spots in selected area diffraction (SAED) confirm the film is nanocrystalline with hexagonal phase of ZnO (h-ZnO) [33, JCPDS Card 36–1451]. Thus, the agglomerated particles as observed from TEM image would be h-ZnO. Fig. 5 shows the XRD pattern of the film having 60% indium concentration cured at 450 °C. The Inset (a) of the figure show the TEM image of the scratched off film with the histogram for particle size distribution and selected area diffraction pattern of the film and Inset (b) shows the EDS data for the presence of different elements in the films network. XRD of films formed by lower indium concentration (i.e., <60%) however shows that the films are crystalline with intensity varying with indium concentration and have been reported in Ref. 30.

B. FTIR vibration and thermal evaluation

FTIR spectral study of the thin film (Fig. 6) cured at three different temperatures (150 °C, 300 °C, and 450 °C) is done to understand the evolution of gel to oxide structure. In case of ZI60 (150 °C) film, a strong vibration appeared at 1642 cm^{-1} assigned to bending mode of adsorbed water [δ (O-H)].[34] The bands at 1348 cm^{-1} and 1390 cm^{-1} are associated with bonded NO_3 and free NO_3 group, respectively,[35,36] whereas the vibrations appearing at 1157 cm^{-1}, 1053 cm^{-1}, and 828 cm^{-1} are attributed to organic moiety (C-H bending in plane and out of plane, CH_2 rocking, C-C bond vibration).[37,38] The vibration related to zinc acetate is found at 672 cm^{-1}.[34,39] In TG-DTA (Fig. 7), it was found that when the film is cured at 150 °C, the mass loss (~17%) is found mainly due to loss of free water[35] as the presence of organics are found by FTIR, while the 1D pattern peak

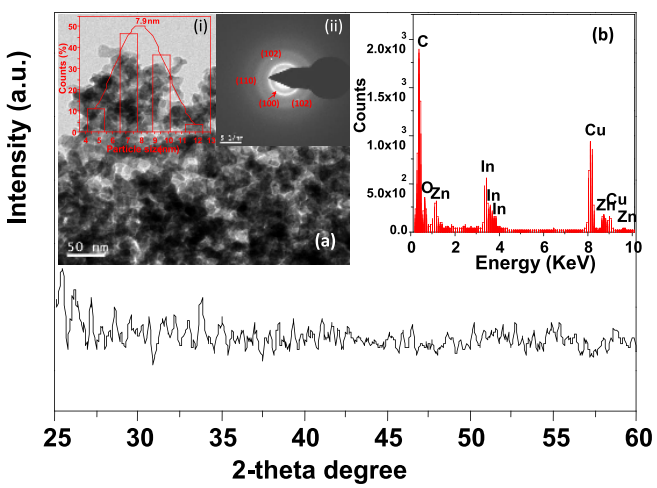

FIG. 5. XRD pattern of the grating film cured at 450 °C. Inset (a) show the TEM image of the scratched off film. Insets (i) and (ii) of inset (a) display the histogram for particle size distribution and selected area diffraction pattern of the film. Inset (b) shows the EDS data for the presence of different elements in the films network.

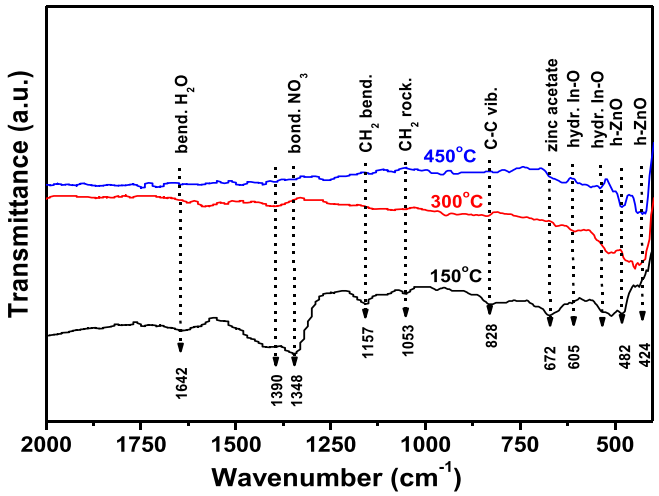

FIG. 6. Substrate corrected FTIR spectra of the ZI60 film formed after curing at three different temperatures.

height is 45 nm as seen in the AFM studies (Fig. 3(a)). However, the film was cured at 300 °C, the organics and water present in the films seemed to be very less as confirmed from nearly disappearance the peaks in the FTIR spectrum. It is also supported by the TG-DTA (Fig. 7) curve where the major mass loss (∼36%) was found at 300 °C in the gels. This could be a reason for decrease in the patterned peak height to 25 nm when the film was cured at 300 °C (Fig. 3(b)). It is important to note that no vibrations for organics was found in the films cured at 450 °C and there was also very low mass loss (∼1%) obtained from the TG-DTA experiment confirmed the fully conversion of gel to oxide networks though the shrinkage of patterned films. The intensity of vibration at 424 cm^{-1} (Ref. 40) and 482 cm^{-1} is found that it increased with increasing curing temperature of the films could be associated with ZnO.[33] It is interesting to note that the appearance of FTIR vibration peaks at 605 and 540 cm^{-1} for the film cured at 300 °C might indicate the presence of In-O stretching vibration.[41]

C. Optical property of the pattern

The film transmittance obtained using a UV-VIS spectrophotometer is shown in Fig. 8. It is seen that the transmission is roughly over 85% throughout the whole visible range. It is also seen that there is a difference in transmission value for patterned and unpatterned films although this difference is insignificant. Possible reason for the decrease of transmission of unpatterned film compared to patterned film is the greater absorption of unpatterned film, whose thickness (∼100 nm) is much more compared to the maximum height of pattern in the patterned film (∼20 nm). The transmission of the bare substrate is also plotted in the figure. The diffraction pattern of the 1D and 2D grating is observed using the standard optical setup shown in Fig. 9(a). The diffraction patterns are seen on a white screen and are then captured using a CCD camera. They are shown in Figs. 9(b) and 9(c) for 1D and 2D gratings, respectively. The neutral density (ND) filter is used in the setup to control the diffracted light intensity. The lens is used to keep the diffraction pattern within the frame of CCD array. The diffraction pattern shows that the ±1 orders are present only. Even faint traces of any higher orders are not noticed. This confirms that the grating is sinusoidal in nature. This sinusoidal nature of the grating is also confirmed from the AFM images. The ±1 orders are not with the same size and shape; this confirms that the master is not perfectly straight line in nature as commercially available CDs are used as master here. The grid within such CD is circular in nature and only a portion of the CD is considered as master here.

D. Electrical property of the pattern

The cut-off wavelengths (CUWs) have been determined from UV-VIS transmission spectra (shown as Inset (i)) of Indium Zinc Oxide patterned films cured at 450 °C and are shown in Fig. 10(a). The CUWs values are 330 nm, 323 nm, 312 nm, and 303 nm for the films derived from 30 (ZI30), 40 (ZI40), 55 (ZI55), and 60 (ZI60) at. % indium containing precursor solutions, respectively. Thus, a blue shifting of the calculated CUWs is observed on increasing indium concentration in the precursor solutions. Further, a plot is drawn to

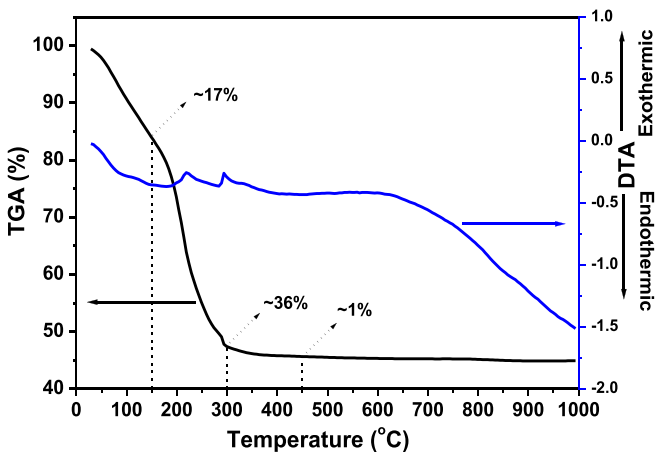

FIG. 7. Plot of TG-DTA analysis data of the ZI60 film.

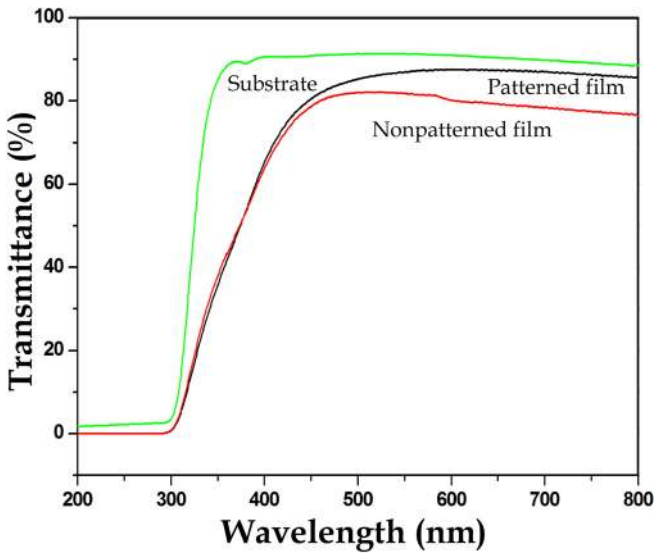

FIG. 8. UV-VIS spectrum of patterned ZI60 film along with that of unpatterned film and the glass substrate used.

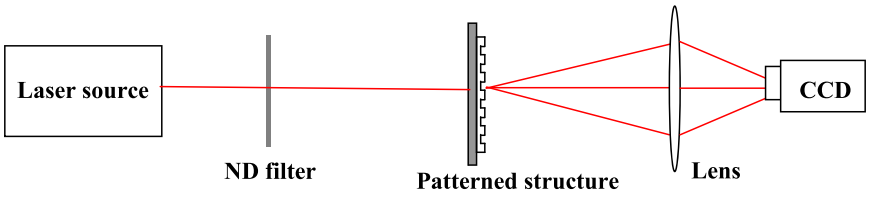

(a)

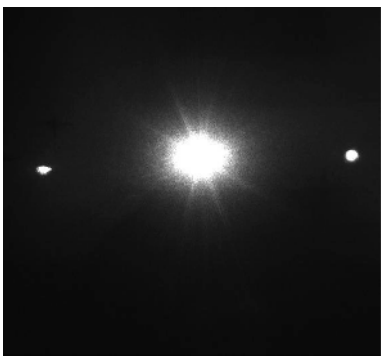

(b)

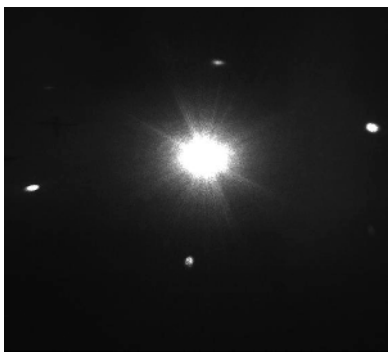

(c)

FIG. 9. (a) Setup used for seeing the diffraction pattern of fabricated grating structures, (b) diffraction pattern of 1D grating, (c) Diffraction pattern of 2D grating.

obtain the change of CUWs with indium concentration and shown in the inset (ii) of Fig. 10(a). The blue shifting of CUWs could be explained[42,43] by the Burstein-Moss effect. In addition, the Sheet Resistance Values (SRV) of the films versus indium content of the precursor solutions are plotted and are shown in Fig. 10(b). It is found that the trend in change of SRV and CUWs with indium concentration is approximately identical. It is also seen that the sheet resistance decreases with increasing indium content of the precursor solution. The increased indium in indium zinc oxide network would increase oxygen vacancy related defects[44] resulting in lowering of the electrical sheet resistance of the films. Relatively high value of sheet resistance than the reported value in the literature[42] would be due to presence of greater extent of film porosity. This would be because the low temperature sol-gel based films are generally porous[45] in nature. Also the sheet resistance drastically reduces as indium concentration is increased. From the best fit curve (4th order polynomial) plotted along with the measured value, it is seen that its sheet resistance becomes comparable with ITO if the at. % of indium concentration is increased slightly above 60% (typical ITO sheet resistance: 10Ω/square[46]). Thus, it can be concluded that the conductivity of the proposed material is very good for TCOs application.

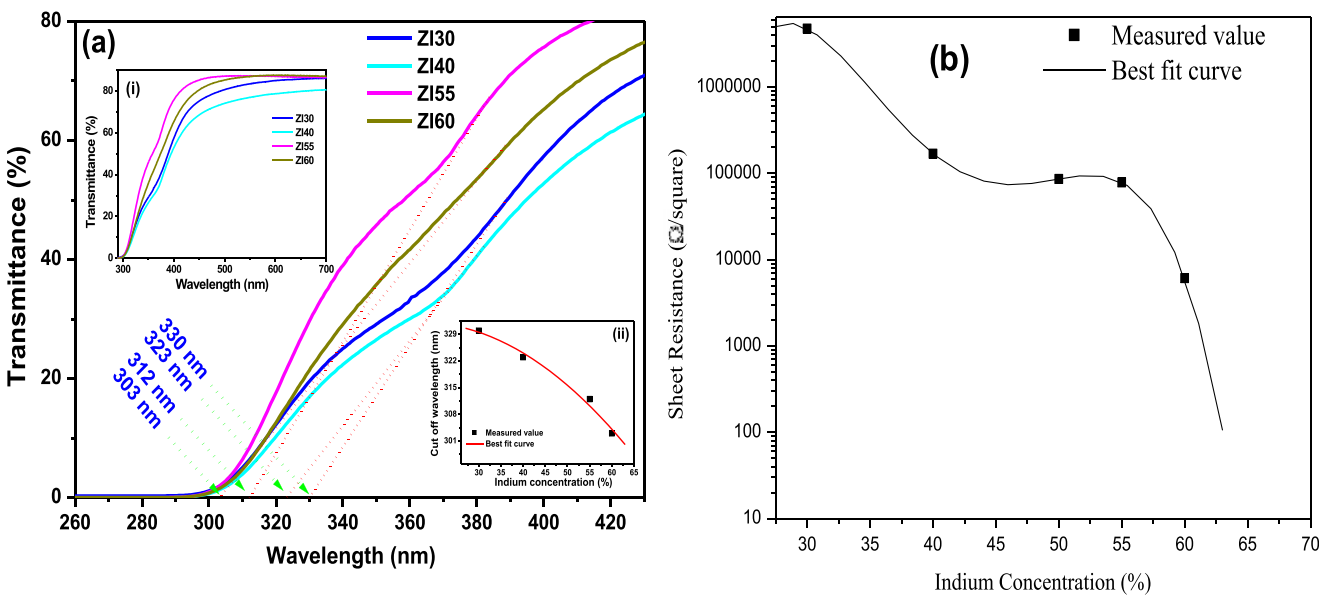

FIG. 10. (a) Determination of cut off wavelengths from UV-VIS transmission spectra of indium zinc oxide patterned films cured at 450 °C. Insets (i) and (ii) show the UV-VIS transmission spectra and the change of cut off wavelengths with indium concentration in the precursor solutions, respectively. (b) Change of sheet resistance with indium concentration in the precursor solutions.

V. CONCLUSIONS

A Transparent Conducting Oxide (TCO) which is indium-zinc oxide (IZO) having 60% Indium have been developed using sol-gel process. Thin films of this TCO can act as top metal contact layer of LED. From XRD studies, it is seen that this particular percentage of Indium gives an amorphous film. With this particular composition, smooth patterned films free from microparticles can be formed and are verified by FESEM and TEM studies. FTIR spectra and TG-DTA thermal evaluation have given the idea of its formation process. Their visible transmission and sheet resistance are comparable to ITO and can therefore compete as its low cost substitute. Smooth 1D and 2D gratings have been patterned on this TCO which can be used to increase light extraction efficiency of LED. Diffraction pattern of the grating structure confirms the sinusoidal nature of its profile. DOEs in the form of Fresnel lens array can also be patterned that can assist in beam shaping of LED output.

ACKNOWLEDGMENTS

The first author (A.H.) is thankful to the Director, CSIR-CGCRI, Kolkata for allowing her to carry out the material development as part of her M.Tech project under the joint supervision of S.J. and R.C. The first three authors (A.H., S.B., and S.J.) acknowledge the Director, CSIR-CGCRI, Kolkata for his kind permission to publish this work. One of author, S.B. also thankfully acknowledges CSIR, for providing his Ph.D. research fellowship under CSIR-NET Fellowship scheme. The work is part of the CSIR funded Supra Institutional Network Project (SINP) (No. ESC0202) of 12th Five Year Plan.

[1]M. R. Krames, O. B. Shchekin, R. Mueller-Mach, G. O. Mueller, L. Zhou, G. Harbers, and M. G. Craford, "Status and future of high-power light-emitting diodes for solid-state lighting," J. Disp. Technol. **3**, 160–175 (2007).
[2]J.-W. Pan, P.-J. Tsai, K.-D. Chang, and Y.-Y. Chang, "Light extraction efficiency analysis of GaN-based light-emitting diodes with nanopatterned sapphire substrates," Appl. Opt. **52**, 1358–1367 (2013).
[3]X. Jin, B. Zhang, T. Dai, W. Wei, X. Kang, G. Zhang, S. Trieu, and F. Wang, "Optimization of top polymer gratings to improve GaN LEDs light transmission," Chin. Opt. Lett. **6**, 788–790 (2008).
[4]A. I. Zhmakin, "Enhancement of light extraction from light emitting diodes," Phys. Rep. **498**, 189–241 (2011).
[5]S. S. Trieu and X. Jin, "Study of top and bottom photonic gratings on GaN LED with error grating models," IEEE J. Quantum Electron. **46**, 1456–1463 (2010).
[6]R. H. Horng, C. C. Yang, J. Y. Wu, S. H. Huang, C. E. Lee, and D. S. Wuu, "GaN-based light-emitting diodes with indium tin oxide texturing window layers using natural lithography," Appl. Phys. Lett. **86**, 221101 (2005).
[7]T. X. Lee, C. Y. Lin, S. H. Ma, and C. C. Sun, "Analysis of position dependent light extraction of GaN-based LEDs," Opt. Express **13**, 4175–4179 (2005).
[8]C. Weisman, K. Bergenek, N. Linder, and U. T. Schwarz, "Photonic crystal LEDs-designing light extraction," Laser Photon. Rev. **3**, 262–286 (2009).
[9]H.-G. Hong, S.-S. Kim, D.-Y. Kim, T. Lee, J.-O. Song, J. H. Cho, C. Sone, Y. Park, and T.-Y. Seong, "Enhancement of the light output of GaN-based ultraviolet light-emitting diodes by a one-dimensional nanopatterning process," Appl. Phys. Lett. **88**, 103505–103507 (2006).
[10]S. M. Huang, Y. Yao, C. Jin, Z. Sun, and Z. J. Dong, "Enhancement of the light output of GaN-based light-emitting diodes using surface-textured indium-tin-oxide transparent ohmic contacts," Displays **29**, 254–259 (2008).
[11]S. Trieu, X. Jin, A. Ellaboudy, B. Zhang, X.-N. Kang, G.-Y. Zhang, X. Chang, W. Wei, S. Y. Jian, and F. X. Xing, "Top transmission grating GaN LED simulations for light extraction improvement," in *Physics and Simulation of Optoelectronic Devices XIX*, edited by B. Witzigmann, F. Henneberger, Y. Arakawa, and A. Freundlich (Proc. of SPIE, 2011), Vol. 7933, p. 79331Y.
[12]X. Jin, S. Trieu, F. Wang, B. Zhang, T. Dai, X. Kang, and G. Zhang, "Design simulation of top ITO gratings to improve light transmission for gallium nitride LEDs," 6th Intl Conf. Information Technology: New Generations, Proc. IEEE Comp. Soc., pp. 1–4, 2009.
[13]J.-H. Song, Y.-C. Leem, Y.-S. Park, H.-M. Lee, W. Lim, S.-T. Kim, G.-Y. Jung, and S.-J. Park, "Light extraction efficiency of GaN-based LEDs with non-periodic and periodic sub-wavelength structures," J. Korean Phys. Soc. **62**, 770–774 (2013).
[14]J. Francés, C. Neipp, S. Gallego, S. Bleda, A. Márquez, I. Pascual, and A. Beléndez, "Comparison of simplified theories in the analysis of the diffraction efficiency in surface-relief gratings," Proc. SPIE **8429**, 84291U–9 (2012).
[15]K. Bao, X. Kang, B. Zhang, T. Dai, Y. Sun, Q. Fu, G. Lian, G. Xiong, G. Zhang, and Y. Chen, "Improvement of light extraction from GaNbased thin-film light-emitting diodes by patterning undoped GaN using modified laser lift-off," Appl. Phys. Lett. **92**, 141104 (2008).
[16]H. Gao, F. Yan, Y. Zhang, J. Li, Y. Zeng, and G. Wang, "Enhancement of the light output power of InGaN/GaN light-emitting diodes grown on pyramidal patterned sapphire substrates in the micro- and nanoscale," J. Appl. Phys. **103**, 014314 (2008).
[17]S. Kim, K. Lee, J. Kim, M. Kwon, and S. Park, "Fabrication of photonic crystal structures on light emitting diodes by nanoimprint lithography," Nanotechnology **18**, 055306 (2007).
[18]D. H. Long, I.-K. Hwang, and S.-W. Ryu, "Theoretical analysis of the light extraction efficiency of a light-emitting diode with a bottom photonic crystal," J. Korean Phys. Soc. **55**, 162–166 (2009).
[19]R.-H. Horng, K.-C. Shen, C.-Y. Yin, C.-Y. Huang, and D.-S. Wuu, "High performance of Ga-doped ZnO transparent conductive layers using MOCVD for GaN LED applications," Opt. Exp. **21**, 14452–14457 (2013).
[20]D. S. Ginley and C. Bright, "Transparent conducting oxides," MRS Bull. **25**, 15–18 (2000).
[21]P. P. Edwards, A. Porch, M. O. Jones, D. V. Morgan, and R. M. Perks, "Basic materials physics of transparent conducting oxides," Dalton Trans. **19**, 2995–3002 (2004).
[22]A. Kumar and C. Zhou, "The race to replace tin-doped indium oxide: Which material will win?," ACS Nano **4**, 11–14 (2010).
[23]C. A. Hoel, T. O. Mason, J.-F. Gaillard, and K. R. Poeppelmeier, "Transparent conducting oxides in the ZnO-In_2O_3-SnO_2 system," Chem. Mater. **22**, 3569–3579 (2010).
[24]C. Battaglia, J. Escarré, K. Söderström, M. Charriére, M. Despeisse, F.-J. Haug, and C. Ballif, "Nanomoulding of transparent zinc oxide electrodes for efficient light trapping in solar cells," Nature Photon. **5**, 535–538 (2011).
[25]S. P. Harvey, K. R. Poeppelmeier, and T. O. Mason, "Subsolidus phase relationship in the ZnO-In_2O_3-SnO_2 system," J. Am. Ceram. Soc. **91**, 3683–3689 (2008).
[26]T. Minami, T. Yamamoto, Y. Toda, and T. Miyata, "Transparent conducting zinc-co-doped ITO films prepared by magnetron sputtering," Thin Solid Films **373**, 189–194 (2000).
[27]N. Naghavi, C. Marcel, L. Dupont, A. Rougier, J.-B. Leriche, and C. Guery, "Structural and physical characterisation of transparent conducting pulsed laser deposited In_2O_3–ZnO thin films," J. Mater. Chem. **10**, 2315–2319 (2000).
[28]A. Wang, J. Dai, J. Cheng, M. P. Chudzik, T. J. Marks, R. P. H. Chang, and C. R. Kannewurf, "Charge transport, optical transparency, microstructure, and processing relationships in transparent conductive indium–zinc oxide films grown by low-pressure metal-organic chemical vapor deposition," Appl. Phys. Lett. **73**, 327–329 (1998).
[29]J. Wienke and A. S. Booij, "ZnO:In deposition by spray pyrolysis—Influence of the growth conditions on the electrical and optical properties," Thin Solid Films **516**, 4508–4512 (2008).
[30]S. Bera, A. Haldar, M. Pal, S. Sarkar, R. Chakraborty, and S. Jana, "Influence of solution composition on periodic surface patterning, morphology and photocatalytic activity of zinc indium oxide thin films," (to be communicated).
[31]S. Sarkar, P. K. Biswas, and S. Jana, "Nano silver coated patterned silica thin film by sol–gel based soft lithography technique," J. Sol-Gel Sci. Technol. **61**, 577–584 (2012).

[32]X. Zhang, W. Que, J. Chen, J. Hu, T. Gao, and W. Liu, "Sol–gel concave micro-lens arrays fabricated by combining the replicated PDMS soft mold with UV-cured imprint process," Appl. Phys. B **113**, 299–306 (2013).
[33]S. Bera, M. Pal, S. Sarkar, and S. Jana, "Dependence of precursor composition on patterning and morphology of sol–gel soft lithography based zinc zirconium oxide thin films," Appl. Surf. Sci. **273**, 39–48 (2013).
[34]R. -Qi. Song, A.-W. Xu, B. Deng, Q. Li, and G.-Y. Chen, "From layered basic zinc acetate nanobelts to Hierarchical zinc oxide nanostructures and porous zinc oxide nanobelts," Adv. Funct. Mater. **17**, 296–306 (2007).
[35]N. Das and P. K. Biswas, "Synthesis and characterization of smoke like porous sol-gel indium tin oxide coating on glass," J. Mater. Sci. **47**, 289–298 (2012).
[36]N. Das, S. Chakraborty, and P. K. Biswas, "Novel polyvinyl alcohol based Cr(III)-Sn(IV) doped In(III) nitrate composite foam: synthesis, unit cell formulation and structure," RSC Adv. **2**, 9183-919 (2012).
[37]N. Giri, R. K. Natarajan, S. Gunasekaran, and S. Shreemathi, "FTIR, ^{13}c NMR and UV visible study of blend behavior of sodium polyacrylate nanosilver composite," World J. Sci. Technol. **1**, 54–61 (2011).
[38]A. J. Kora and J. Arunachalam, "Green fabrication of silver nanoparticles by gum tragacanth (Astragalusgummifer): A dual functional reductant and stabilizer," J. Nanomater. **2012**, 765–869.
[39]S. Bhattacharyya and A. Gedanken, "A template-free, sonochemical route to porous ZnO nano-disks," Microporous Mesoporous Mater. **110**, 553–559 (2008).
[40]S. Mallakpour and M. Madani, "Use of silane coupling agent for surface modification of zinc oxide as inorganic filler and preparation of poly(amide–imide)/zinc oxide nanocomposite containing phenylalanine moieties," Bull. Mater. Sci. **35**, 333–339 (2012).
[41]T. Sato, "Preparation and thermal decomposition of Indium Hydroxide," J. Therm. Anal. Calorim. **82**, 775–782 (2005).
[42]S.-M. Kim, H.-W. Choi, K.-H. Kim, S.-J. Park, and H.-H. Yoon, "Preparation of ITO and IZO thin films by using the facing targets sputtering (FTS) method," J. Korean Phys Soc **55**(5), 1996–2001 (2009).
[43]I. Hamberg and C. G. Granqvist, "Evaporated Sn-doped In_2O_3 films: Basic optical properties and applications to energy-efficient windows," J. Appl. Phys. **60**, R123 (1986).
[44]M. P. Taylor, D. W. Readey, M. F. A. M. v. Hest, C. W. Teplin, J. L. Alleman, M. S. Dabney, L. M. Gedvilas, B. M. Keyes, B. To, J. D. Perkins, and D. S. Ginley, "The remarkable thermal stability of amorphous In-Zn-O transparent conductors," Adv. Funct. Mater. **18**, 3169–3178 (2008).
[45]S. Jana and P. K. Biswas, "Effect of Zr(IV) doping on the optical properties of sol-gel based nanostructured indium oxide films on glass," Mater. Chem. Phys. **117**, 511–516 (2009).
[46]J. M. Phillips, R. J. Cava, G. A. Thomas, S. A. Carter, J. Kwo *et al.*, "Zinc-indium-oxide: A high conductivity transparent conducting oxide," Appl. Phys. Lett. **67**, 2246–2248 (1995).